The above calculations have all been done under the assumption of constant input displacement. For the first cavity this will be essentially correct, but for subsequent cavities the deflected beam transverse position will change as the transverse fields build up. Since is proportional to L^2, it is of concern whether several cavities do not indeed act as a long cavity and lead to a reduced starting current. This is not the case for the following reasons.

If the current is less than the starting current in the first cavity, the field and transverse displacement will ultimately reach a finite value. In the second cavity one then has, at worst, a driving term of bounded magnitude and the stability will once again depend only on the homogeneous part of Eq. [1]. Consequently the stability limits for the group of cavities are those for the individual cavities. However, it can be expected that the transverse amplitude under these conditions will be larger in successive cavities, particularly where there is a harmonic resonance between the beam pulse frequency and a transverse mode. This resonance condition has a width of order ε and therefore is not likely to occur in more than one cavity.

A second factor limiting the growth of transverse displacement is the presence of a transverse focusing system. This will limit the effective cavity length to approximately $\lambda/2\pi$, where λ is the transverse oscillation wavelength and is therefore an additional deterrent to cooperative action between tanks.

Calculations are in progress to confirm these and other assertions about the interaction of the beam with transverse cavity modes. At present it appears that the current limits for these effects are of order 10 amperes for the Brookhaven and Los Alamos linear accelerators, safely above the design currents.

REFERENCES

(1) See, for example, P. B. Wilson, HEPL Report No. 297, Stanford (1963).
(2) R. L. Gluckstern: Brookhaven Report AADD-38, (1964); MURA Conf. on Linear Accelerators, Stoughton, 1964, p. 186.
(3) R. L. Gluckstern and H. S. Butler: IEEE Trans. on Nuclear Science, *NS-12*, no. 3, p. 607 (1965).

DISCUSSION

MONTAGUE: I am puzzled by your conclusion that the effect is independent of whether the transverse mode is a forward or backward wave, for two reasons.

a) The dispersion diagram you illustrated is for a backward wave; the forward wave with the same bandwidth would intersect the v = c line in the 2nd Brillouin zone at a larger angle, and the phase velocity difference would be greater.

b) It has been generally believed that a backward wave is more serious than a forward wave, because the energy in the transverse mode travels backwards to influence the later beam entering the accelerator section.

GLUCKSTERN: a) For structures now being considered, the width of the transverse band is quite small (few percent) and the angle of intersection of the beam velocity line with the band is not greatly different in the forward or backward wave region.

b) The designation of forward or backward wave is relevant primarily to traveling wave structures, where your statement certainly is true. But for standing wave structures there are both forward and backward waves in each mode, which are not related in the same way to the slope of the dispersion curve. The beam picks out that wave component with which the interaction is most serious.

SCHOPPER: Is the critical current proportional to the inverse of the Q value and would it therefore be correspondingly decreased for a superconducting linac?

GLUCKSTERN: Yes, so the current limit would be very small. It may however be possible to arrange for the accelerating mode to be superconducting, but for the transverse modes to generate fields in a normally conducting region.

NORMAL MODE ANALYSIS OF STANDING WAVE LINACS *

T. Nishikawa**

Brookhaven National Laboratory, Upton, New York (USA)

For the acceleration of protons, most linacs use a standing wave configuration similar to that of the TM_{01n} mode in a cylindrical cavity. Field distribution in such a long cavity is determined by the wave propagation under wall losses, beam loading, and other perturbations. Using microwave cavity theory (1) the actual field, $\vec{E}$ (z, r, θ, t),

* Work performed under the auspices of the U.S. Atomic Energy Commission.
** On leave from the University of Tokyo, Tokyo, Japan.

can be expressed in terms of the normal mode functions,

$$\vec{E}\ (z, r, \theta, t) = \sum_n V_n(t)\ \vec{E}_n\ (z, r, \theta). \qquad [1]$$

The normal modes, $\vec{E}_n$ (z, r, θ), form a complete orthogonal set of functions which are obtained from the field in an ideal cavity bounded by perfectly conducting and perfectly insulated surfaces. If the cavity is excited near one of the normal mode frequencies, ω_l (n = 1), the modes near the l^{th} mode predominate in the normal mode analysis; these modes have a different z-dependence from the resonant mode but the axial field will have the same radial and azimuthal dependences. The axial component of the n^{th} normal mode of an Alvarez cavity can be written thus

$$E_n(z) = \frac{E_o}{\sqrt{\tau_n}} \cos\frac{n\pi z}{L},\quad n = 0, 1, 2, \ldots (l = 0) \qquad [2]$$

where L is the cavity length, E_o is a function of r but independent of z, and τ_n (= 2 for n = 0 and 1 for n ≠0) is a normalization factor. For a loosely coupled multicell cavity of (N-1) uniform cells (cell length L_o) and two end cells of half length, the normal mode field will be

$$E_n(m) = \frac{E_o}{\sqrt{\tau_n}} \cos m\frac{n\pi}{L} \qquad [3]$$

at the m^{th} cell (τ_n = 2 for n = 0, N, ... and 1 for others). Fields given by [2] and [3] have similar forms; both have orthogonal relations between different n's, satisfy boundary conditions at end walls, and are verified by measurements (2, 3).

Using Maxwell's equations, the coefficient V_n (t) in [1] is given by (1)

$$\frac{d^2}{dt^2} V_n + (1 + j)\frac{\omega_n}{Q_{on}}\frac{d}{dt} V_n + \omega_n V_n^2 =$$

$$= \frac{1}{\varepsilon}\left[\frac{d}{dt}\int_{s'} (\vec{H} \times \vec{E}_n)\,\vec{n}\,ds - \frac{d}{dt}\int_v \vec{J}\cdot\vec{E}_n\,dv\right] \qquad [4]$$

where the effect of wall losses has been included in the left side by means of the standard evaluation of Q_{on}. The first term on the right side gives the driving force due to the external power source which is coupled to the cavity through a surface S'; the normal mode arises when there is an open circuit at S'. The last term is the driving force due to a beam having current density, J, inside the cavity. The components of the field excited by the generator and induced by beam can be derived separately and later added to obtain the total field with beam loading.

1. FIELD EXCITED BY A WELL-PADDED GENERATOR

If we can assume a well-padded generator as a power source, the equation of cavity oscillation at the l^{th} resonance becomes

$$\frac{d^2}{dt^2} V_n + (1 + j K_n)\frac{\omega_n}{Q_n}\frac{d}{dt} V_n + \omega_n^2 V_n =$$

$$= h U_n e^{j\omega_l t} - (1 - \delta_{n,l})\frac{U_n}{U_l}\frac{\omega_l}{Q_{ext,l}}\frac{dV_l}{dt}, \qquad [5]$$

where the loaded and external Q's have a relation $1/Q_n = 1/Q_{on} + 1/Q_{ext,n}$. U_n is a coupling coefficient between the n^{th} normal mode of the cavity and the input waveguide mode. The l^{th} mode resonant frequency is $\omega_l' \approx \omega_l (1\text{-}1/2Q_{lo})$.

The procedure to derive [5] from [4] will be presented elsewhere (4). We note here only that the incident wave is $\frac{1}{2}\, hU_n e^{j\omega_l t}$ and the reflected wave depends on $\sum_n dV_n/dt \approx DV_l/dt$.

For a step function incident wave, the field of the resonant mode (n =l) is

$$E_o e^{j\omega_l' t}\left[1 - e^{-\frac{\omega_l'}{2Q_l}t}\right]\cos\frac{l\pi z}{L}, \qquad [6]$$

where E_o is $h\ E_o\ Q_l\ U_l / j\sqrt{\tau_l\ \omega_l'^2}$. For a nonresonant mode (n ≠ l), the field is

$$j E_o \frac{\omega_l'^2}{Q_l(\omega_n'^2 - \omega_l'^2)}\sqrt{\frac{\tau_l}{\tau_n}}\frac{U_n}{U_l} e^{j\omega_l' t}\left[1 - \frac{Q_l}{Q_{ext.\,l}}\right.$$

$$\left.\left(1 - e^{-\frac{\omega_l'}{2Q_l'}t}\right) - e^{-\frac{\omega_n'}{2Q_n'}t}\, e^{j\left(\omega_n' - \omega_l'\right)t}\right]\cos\frac{n\pi z}{L} \qquad [7]$$

assuming that $\omega'_l\,\omega'_{ln}/Q_n \ll |\,\omega_l'^2 - \omega_l'^2\,|$. Equation [6] gives a usual build-up curve of cavity resonance. From [7], the amplitude of nonresonant modes is proportional to $1/\Omega_{ln}$ (where $\Omega_{ln} = |\,\omega_n' - \omega_l'\,|$) and, in general, decreases rapidly as n increases. In a transient state, the nonresonant term shows wiggles having the angular frequency Ω_{ln}, which arise from the beat between the free oscillation of that mode and driving force. The amplitude of wiggles changes along the z axis in the same

manner as the axial component of the n^{th} mode, and dies out in the steady state where the non-resonant mode becomes 90° out of phase with the resonant mode.

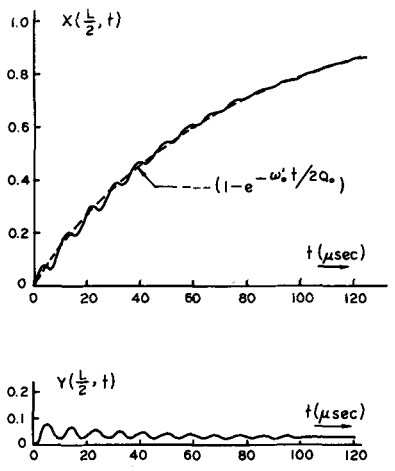

Fig. 1 - Normalized real and imaginary parts of field at center of AGS linac cavity (calc.).

2. FIELD INDUCED BY THE BEAM

Assuming a tightly bunched beam, the field induced by the beam is given by the last term of [4],

$$\frac{1}{\varepsilon}\frac{d}{dt}\int \vec{J}\cdot\vec{E}_n\,dv. \qquad [8]$$

After integration, the induced field becomes negligible except for the synchronized mode for which the particle velocity v_o satisfies the relation, $\omega'_l = k_l v_o$.* At the axis, the l^{th} mode field induced by the beam is

$$E_{bl}(z, t') = -r_e I_o f(\delta\varphi)\frac{Q_l}{T_l Q_{ol}} e^{j(\omega_l t' + \varphi_b)} \cdot \left(1 - e^{-\frac{\omega'_l}{2Q_l}t'}\right)\cos\frac{l\pi z}{L} \qquad [9]$$

Here r_e is the effective shunt impedance, I_o the average beam current, T_l the transit time factor, φ_b the stable phase angle, and $f(\delta\varphi)$ the form factor of beam having a phase spread of $\delta\varphi$. It is assumed that all beam parameters are constant over the length. The induced field is in the opposite phase to that of the beam bunches, and builds up from $t' = t - t_o = 0$ by writing the time of beam arrival as t_o.

* Initially, while the beam is filling the cavity, this argument is slightly different (4).

3. RESULTS OF ANALYSIS

a) Scallops and delay time in a transient

It is now possible to calculate the real and imaginary parts of the transient field. Fig. 1 shows the calculated values at the center of the AGS linac. Since the TM_{011} mode is hardly excited due to the center feed ($U_n \approx 0$ for odd n), and since the effect of higher modes ($n > 3$) is a small correction, only the excitation of the Tm_{012} mode is taken into account. Except for an initial period, the calculated real part is immediately compared with the field pattern in Fig. 2 which is observed by a pick-up electrode. For small t, the imaginary parts also are appreciable; Fig. 3 shows the calculated results for the center (driving point) and the far ends of the cavity. The delay time of field build-up at the far ends can be approximated thus (4), $t_d \approx \pi/2\Omega_{o2}$, which is about 2.2 μsec for the AGS linac. If we consider the

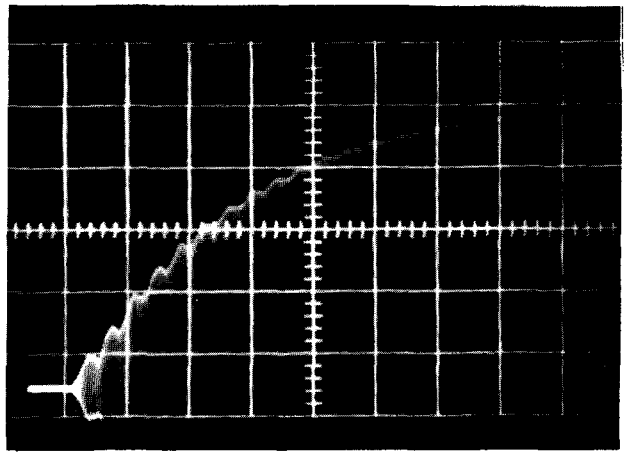

a)

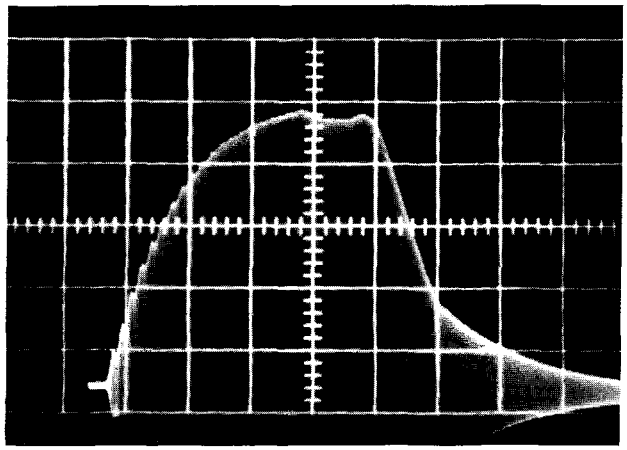

b)

Fig. 2 - R.f. field pattern near the center of AGS cavity. a) initial build-up (20 μs/div); b) full pulse showing remaining effect after beam loading compensation (50 μs/div).

excitation of the TM_{011} mode, then we get an asymmetry i nthe delay times at the ends of a center coupled cavity, the order of which will be 0.1 μsec for the AGS linac. Measurements by Keane (5) on the AGS linac cavity give observed values between 1.5 and 2.5 μsec at both ends (almost symmetric for each end).

Fig. 4 shows the measured transient build-up for a π-mode multicell cavity (6); agreement with Fig. 3 is excellent except for differences due to different parameters.

b) Phase shift at a cut-off mode

The zero-mode Alvarez cavity and the π-mode multicell cavity have nonlinear dispersion relations. For these cases, energy flow involves nearby modes with additional phase shifts. Using Eq. [7] and $\Omega_{ln} \propto (n-l)^2$, the steady-state phase shifts are proportional to L^2/Q_{lo}; they are also close to the results by equivalent circuit analyses (7). The calculated phase shift for an Alvarez cavity will be of the order of one degree; for a π-mode multicell cavity it is of the order of ten degrees. With beam, these phase shifts increase corresponding to the energy dissipated into beam. Therefore, the π-mode structure is extremely sensitive to beam loading (8).

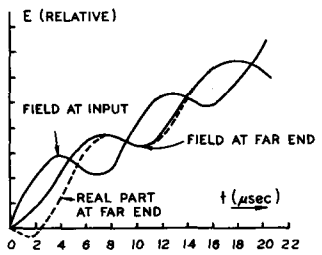

Fig. 3 - Calculated field amplitude at an initial period of AGS linac cavity (both at input and far end).

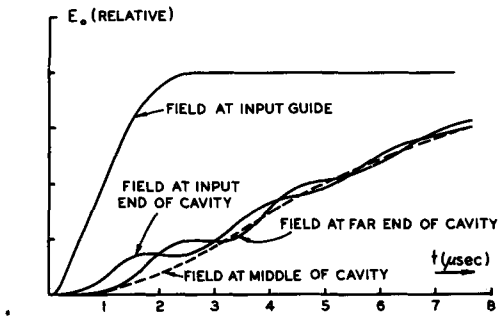

Fig. 4 - Observed field patterns with a π-mode multiple-cell cavity (by S. Giordano) (f_o = 880 Mc, bandwidth = 2.7 Mc, Q = 16,000 and N = 4).

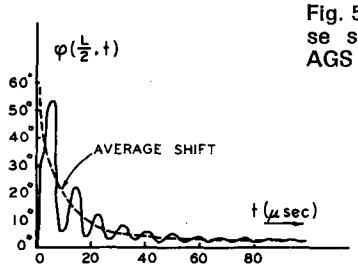

Fig. 5 - Calculated phase shift at center of AGS linac cavity.

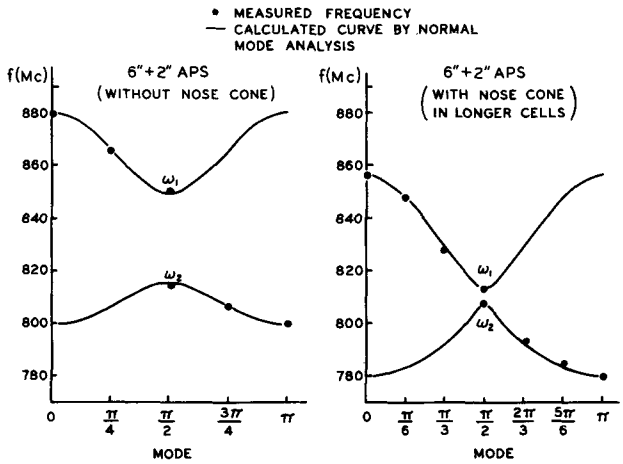

Fig. 6 - Dispersion curves for alternating periodic structures.

The calculated phase shift at a transient oscillates around a phase shift averaged over beat frequencies which is inversely proportional to loaded Q, Q_o, at $t \approx 0$, and unloaded Q, Q_∞, at $t \to \infty$ (Fig. 5) (9).

c) π/2-mode in multicell cavity and alternating periodic structure

If a uniform multicell cavity is operated in the middle of a passband or in the π/2 mode (l = N/2), the resulting field distribution becomes different from that of a cut-off mode. A symmetric frequency distribution of nearby modes around that mode cancels out a part of nonresonant mode effects. Thus, for both a steady and a transient state, any additional phase shift does not appear as a first order effect (4). In the same manner, the effect of tuning errors in each cell will be reduced (8). The only disadvantage to using this mode is a relatively low shunt impedance than the π mode. A new multiple cell structure having an alternating periodicity has been proposed by Giordano (10). In the APS (alternating periodic structure), the length of odd-numbered cells in a uniform structure, where the fundamental mode field is zero at the π/2 mode, is shortened compared with the length of even-numbered cells. An optimum shunt impedance for a π/2 mode (in a traveling wave mode) is obtained at a ratio of cell lengths between three and five.

A calculated dispersion curve (11, 12) for the APS is shown in Fig. 6 with the measured points. The APS mode is essentially a cut-off mode and has two different frequencies, ω_1 and ω_2, corresponding to two field configurations under different boundary conditions (Fig. 7). Between ω_1 and ω_2 there is a stop band; in general, however, by means of a slight change in the boundary of one of the two cell types, one can make ω_1 close enough to ω_2. A very asymmetric dispersion curve (Fig. 7b) is obtained, so that the resonant mode, ω_1, can be separated far enough from its nearest modes (ω_2 cannot exist in an actual cavity). A factor of insensitiveness to beam loading or other perturbations in the APS is given by $|\omega_1 - \omega_2| / \omega_B$ with the total passband width ω_B (12).

d) Compensation of beam loading

In an Alvarez cavity, the beam loading is a transient phenomenon if the beam pulse length, t_b, is shorter than the build-up time. From Eq. [9],

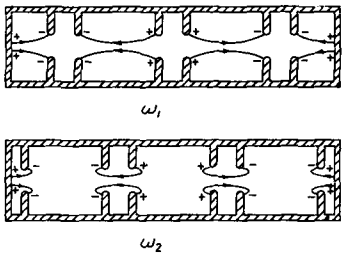

Fig. 7 - Two field configurations in APS corresponding to different boundary conditions.

the maximum decrease in the field strength at the axis is

$$\Delta E_b \cong \frac{r_e J_0 \omega_0' f(\delta\varphi) \cos\varphi_b}{2 Q_\infty T_0} t_b, \qquad [10]$$

which is about 0.1 MV/m for a 20 mA, 20 μsec beam. To obtain a good energy spectrum, beam loading compensation is often used. Compensation can be achieved for the resonant or synchronized mode, but not for the higher modes. As discussed above, the beam gives very small excitation to nonsynchronized modes, whereas a generator excites nearby modes. Since the higher modes have the same phase near the driving point, the compensation will be difficult in that region; this is experienced in the AGS linac. A similar discussion has been given by Lapostolle (13) based on a dielectric waveguide model; his result of L^2-dependence in this effect is again expressed in terms of Ω_{1n} in the normal analysis. The multiple feeds for a long cavity have some advantages; e.g. if the cavity is excited at two points, $z = L/4$ and $3L/4$, then we can raise the nearest higher modes excited to $n = 1 \pm 4$ (TM_{214} mode in an Alvarez cavity).

The author would like to express his thanks to Dr. John P. Blewett for his interest throughout this work and for the hospitality of the Brookhaven Laboratory. He is also grateful to Messrs. S. Giordano and J. T. Keane for experimental information and for helpful discussions.

REFERENCES

(1) J. C. Slater: Microwave Electronics, (D. Van Nostrand, New York, 1950), Chap. 4, p. 57.
(2) J. T. Keane: Minutes of the 1964 Conference on Proton Linear Accelerators, MURA-714 (1964), p. 398.
(3) R. Beringer and R. L. Gluckstern: Yale Report Y-9 (1964).
(4) T. Nishikawa, Brookhaven Report AADD-87 (1965).
(5) J. T. Keane: private communication.
(6) S. Giordano: private communication.
(7) D. E. Nagle and E. A. Knapp: Minutes of the Conference on Proton Linear Accelerators at Yale University, p. 171 (1963); H. J. Hereward: CERN Report MPS/DL Int. 65-1 (1965).
(8) T. Nishikawa: IEEE Trans. on Nuclear Science *NS-12*, No. 3, 630 (1965).
(9) On an equivalent circuit analysis, refer to R.A. Jameson, Minutes of the 1964 Conf. on Proton Linear Accelerators, MURA-714 (1964), p. 505.
(10) S. Giordano: IEEE Trans. on Nuclear Science *NS-12*, No. 3, 213 (1965).
(11) J. P. Blewett: Brookhaven Report AADD-65 (1965).
(12) T. Nishikawa, S. Giordano and D. Carter: Brookhaven Report AADD-88 (1965).
(13) P. M. Lapostolle: CERN Report AR/Int. SG/65-9 (1965).

DISCUSSION

NAGLE: These results are very interesting. The calculation and experimental verification of the response of the iris loaded tank was reported by R. Jameson (MURA Conf. 1964 and PhD Thesis 1965). The explanation was given then of the scalloped response show in prof. Nishikawa's slide, in terms of the interference of the normal modes. The phase shift and amplitude response was calculated.